A Spreading Technique for Forming Film in a Captive Bubble

Günther Putz,* Monika Walch,* Martin Van Eijk,# and Henk P. Haagsman#
*Department of Anaesthesia and Intensive Care Medicine, The Leopold Franzens University of Innsbruck, A-6020 Innsbruck, Austria, and #Laboratory of Veterinary Biochemistry and Institute of Biomembranes, Utrecht University, 3508 TD Utrecht, the Netherlands

ABSTRACT Mechanisms underlying the surface properties of lung surfactant are extensively studied in in vitro systems such as the captive-bubble surfactometer (CBS), the pulsating-bubble surfactometer, and the Wilhelmy balance. Among these systems, the CBS is advantageous when a leakproof system and high cycling rates are required. However, widespread application of the CBS to mechanistic studies of dynamic surfactant protein-phospholipid interactions of spread film and to comparative studies between spread and adsorbed film is hampered because spreading of film is difficult. In addition, when film is formed by adsorption, the amount of material required is fairly large. We have developed an easy spreading technique that allows routine formation of film by spreading of small amounts of surfactant components at the air-water interface of an air bubble in a CBS. The technique is reliable, precise, and accurate, and the biophysical activity of film formed by spreading is similar to that of film formed by adsorption. This method will be useful for mechanistic studies of surfactant components under dynamic conditions and for comparative studies of spread films and adsorbed films.

INTRODUCTION

In the lungs, a surfactant film is formed during inspiration by adsorption of surfactant components from the alveolar subphase to the air-water interface. Upon compression during expiration, these components lower the surface tension at the interface to nearly zero (reviewed in Goerke and Clements, 1986; Goerke and Schürch, 1997). Mechanisms underlying these essential processes for adequate lung function have been extensively studied in in vitro systems such as the captive-bubble surfactometer (CBS), the pulsating-bubble surfactometer, and the Wilhelmy balance. The results obtained with these in vitro systems have substantially increased our understanding of the role that various components play during formation and subsequent compression and expansion of surfactant film.

Among these systems, the CBS is advantageous for investigating the surface activity of a surfactant film formed by adsorption when a leakproof system and high rates of cyclic area changes are required (Schürch et al., 1989; Putz et al., 1994b; Herold et al., 1996). However, in the CBS, spreading of film is difficult. Special equipment is required (Schürch et al., 1989); otherwise, sample handling and spreading of surfactant are tricky (Putz et al., 1994a). As a result, widespread application of the CBS to mechanistic studies of surfactant protein-phospholipid interactions of spread film and to comparative studies of adsorbed and spread film is hampered. In addition, when film is to be formed by adsorption, the amount of surfactant required is fairly large. Because isolation of surfactant components (for example, surfactant proteins) from lungs and expression systems is labor intensive and yields are small, shortage of surfactant potentially becomes a limiting step for repeat experiments.

By reconstructing the CBS and refining the spreading technique by using a syringe instead of a microbore tube or a micromanipulator, we have developed an easy spreading technique that allows routine formation of film by spreading small amounts of surfactant components at the air-water interface of an air bubble in a CBS.

Received for publication 18 February 1998 and in final form 27 July 1998.

Address reprint requests to Dr. Günther Putz, Universitäts klinik für Anaesthesie und Allgemeine Intensivmedizin, Anichstrasse 35, A-6020 Innsbruck, Austria. Tel.: 512-504-4636; Fax: 512-504-4683; E-mail: guenther.putz@uibk.ac.at.

0006-3495/98/11/2229/11 $2.00

MATERIALS AND METHODS

Materials

Materials were purchased from the following manufacturers: 1,2-dipalmitoyl-*sn*-glycero-3-phosphocholine (DPPC), 1-palmitoyl-2-oleoyl-*sn*-glycero-3-(phospho-*rac*-(1-glycerol)) (POPG), 1-oleoyl-2-hydroxy-sn-glycero-3-phosphocholine (LPC), and palmitic acid (PA) from Avanti Polar Lipids (Alabaster, AL); HEPES, EDTA, calcium chloride, potassium chloride, and sodium chloride from Sigma-Aldrich (Vienna, Austria); chloroform ($CHCl_3$) and methanol (MeOH) (HPLC grade) from Burdick and Jackson (Muskegon, MI); and isopropyl alcohol and triethylamine from Fluka Chemie AG (Buchs, Switzerland). These materials were used without further purification. Agarose (SeaKem ME agarose; FMC BioProducts, Rockland, ME) and silicone rubber gaskets (Cal-Neva Supply, Oakland, CA) were extracted as previously described (Putz et al., 1994b). Water used for chemical analyses was filter purified (resistivity > 18 MΩ/cm; Modulab ModuPure; U.S. Filter Corporation, Lowell, MA), and for surface activity measurements it was also quartz distilled (resistivity > 10 MOΩ/cm; Muldestor, Wagner and Munz, Munich, Germany). Silica gel plates (LK5D; Whatman, Clifton, NJ) were activated at 200°C for 30 min, and bands were visualized by spraying (8-anilino-napthalene-1-sulfonic acid, Fluka; and Phospray, Supelco, Bellefonte, PA).

Method development

To allow routine formation of a film by spreading and to improve overall performance, we reconstructed the pressure-driven CBS (Putz et al., 1994a) and then refined the spreading technique.

Reconstruction of pressure-driven CBS

In the reconstruction, several improvements were made to allow routine formation of film (Fig. 1). To provide easy access to the inside of the cuvette for spreading of film, the rear wall of the plexiglas enclosure was screwed onto a split brass beam. To aid in centering the bubble, positioning the needle tip during spreading of film, and checking the bubble's axisymmetry, a second video camera was mounted on top of the plexiglas enclosure. To achieve adequate lighting of the bubble for both side viewing and top viewing, a fiberoptic light source (Cambridge Instruments, Buffalo, NY) was used to illuminate the sample chamber. To avoid disturbing the bubble during stirring, the subphase (sample volume, 0.7 ml) was agitated by a stir bar (Spinbar; Bel-Art Products, Pequannock, NJ) rotating horizontally at the bottom of the sample chamber. To provide undistorted viewing of the bubble contour from the top, the top piece of the cuvette holder was made of glass (Swarovski, Wattens, Austria), and the glass cuvette used was optically clear at the bottom (101-OS; Hellma Cells, Forest Hills, NY). To provide access to both the subphase and the bubble's air-water interface, the rubber gasket was pierced by two polyethylene tubes (PE-160; Intramedic, Clay Adams, Parsippany, NJ). One tube (5 cm long), located in the center of the gasket, was used in spreading experiments to form the bubble and spread film at the bubble air-water interface. It was also used to drain the perfusate and inject lipid vesicles. During changes in cuvette pressure it was sealed with a surgical clamp. The other tube, located in the front corner of the cuvette (30 cm long), was used in adsorption experiments to form the bubble. It was also used to perfuse the sample chamber and change the cuvette pressure.

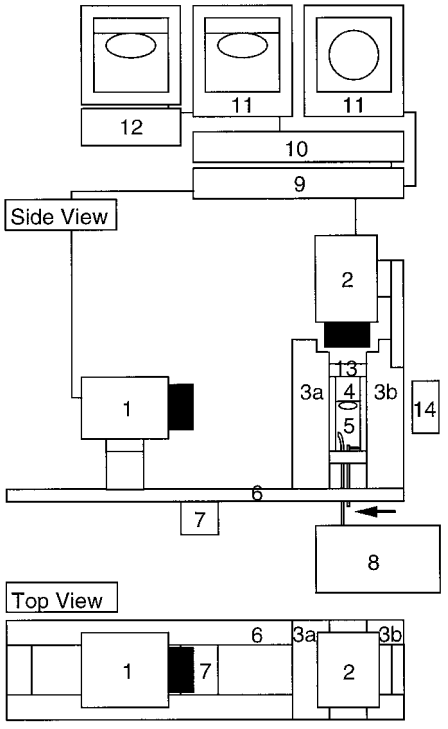

FIGURE 1 Schematic drawing of the improved reconstruction of the pressure-driven captive-bubble surfactometer (not drawn to scale; the pressure device is normally placed at the side of the plexiglas chamber). The rear wall of the plexiglas enclosure is screwed onto a split brass beam to provide access from underneath to the cuvette inside through polyethylene tubing. The split beam is mounted on a ball-and-socket joint to allow unrestricted angular movement of the assembly. A second video camera is mounted on top of the plexiglas enclosure for centering the bubble and checking its axisymmetry. 1, Video camera and lens used for viewing the bubble from the side. 2, Video camera and lens used for viewing the bubble from the top. 3a, Removable front wall. 3b, Nonremovable rear wall of the plexiglas enclosure. 4, Agarose ceiling. 5, Sample chamber with a bubble in aqueous suspension, two polyethylene tubes (for bubble injection, spreading of film, drainage of perfusate, and changing of cuvette pressure), and a horizontally rotating stir bar. 6, Split brass beam. 7, Ball-and-socket joint. 8, Pressure device. 9, Video mixing console. 10, Videotape recorder. 11, TV monitor. 12, Computer plus monitor. 13, Glass top of the cuvette holder. 14, Fiberoptic light source. For clarity, the removable center piece (spacer with recess to hold cuvette) of the plexiglas enclosure, screws used to secure the top and bottom pieces of the cuvette holder, heating elements, and the thermistor needle probe are not shown.

Three additional changes were made to improve the overall performance of the CBS. First, to exclude any release of surface active contaminants from the rubber gasket and their adsorption to the bubble's air-water interface, the rubber gasket is brushed with detergent (Deconex 15PF; Borer AG, Zuchwil, Switzerland), rinsed with distilled water, and covered with a layer of extracted agarose.

Second, the bubble is continuously viewed with two video cameras (Pulnix, Sunnyvale, CA). The top-view camera (TM-7CN) synchronizes the side-view camera (TM-7EX). A 50-mm lens is attached to each camera (21 HA; Tamron, Tokyo, Japan). The lens settings for the side view with a 30-mm spacer ring are f8 and focal length infinity. For the top view with a 10-mm spacer ring they are f8 and focal length 0.7 m. Images are displayed on two TV monitors (12VM1050, Dotronix, New Brighton, MN; VM-903U, Shiba, Tokyo, Japan). A video mixing console (VTM-1; General Service Electronics, Mainz, Germany) is used to switch between the two cameras. Images from one camera at a time can be recorded on a videotape recorder (EVO-9800A; Sony, Teaneck, NJ). Single frames, from the side or from the top, are captured directly or from tape with a frame grabber (RasterOps 24MxTV; Santa Clara, CA) and are stored in a Macintosh Quadra 800 computer (Apple, Cupertino, CA). Stored frames are loaded into an image processing and analysis program (Image, version 1.55), which allows measurements of bubble height and diameter in pixels. A distance of 0.1 cm corresponds to 63 pixels. From the height and the diameter, both the surface tension at the bubble's air-water interface and the area of the bubble are calculated according to the method of Schoel et al. (1994).

Third, to automate cyclic area changes in the bubble's area, a pressure device was built. This pressure device allows rapid area changes between preset limits of cuvette pressure (p) (adjustable restrictors 47.220; Kuhnke, Vösendorf, Austria) by time-controlled operation (square-wave generator) of a solenoid valve (A73; Stasto, Innsbruck, Austria). For $p < 1.0$ absolute atmospheric pressure (ata), a vacuum pump (Divac 2.4 L; Leybold, Köln, Germany) is used. For $p > 1.0$ ata, the compressed air line is used. One problem we noted was that the rise in cuvette pressure from below to above 1.0 ata was too fast. As a result, liquid was pushed into the cuvette so rapidly that turbulence inside the cuvette displaced the bubble and sometimes shattered it. Inserting a reservoir into the pressure circuit solved this problem.

Refinement of the spreading technique

In the reconstructed CBS a bubble (0.5 cm^2) is formed in subphase buffer (140 mM NaCl, 10 mM HEPES, 0.5 mM EDTA, 2.5 mM $CaCl_2$, pH 6.9) by injecting air (29 μl) from a glass syringe (805; Hamilton, Bonaduz, Switzerland) into the sample chamber at 1.0 ata and 37°C while the plexiglas enclosure is in the perpendicular position. After being centered, the bubble is rapidly compressed (~54% area reduction), and surface tension is measured to ensure that the surface is not contaminated before spreading of film. Film is spread only on bubbles with a surface tension equal to or greater than 68 mN/m. Then the sample chamber is illuminated by shining light from a halogen desk lamp (50 W) onto the surface of the rubber gasket to ease visualization of the needle tip from the top. The next step is to spread a solution along the bubble's air-water interface to form a film. The solution consists of surfactant components (phospholipids, proteins) dissolved in an organic solvent, which serves as a spreading agent.

The main refinement of the spreading technique is that film is spread from a conventional positive displacement-type glass syringe with a blunt

tip (7000.5, point style no. 3 needle and Chaney adapter; Hamilton). The blunt tip of the syringe is important because, in contrast to a sharp tip, the blunt tip guarantees reliable contact with the bubble's apex, which makes reproducible spreading possible. This technique is simpler than the previous techniques—spreading from a syringe mounted on a micromanipulator, which is expensive, or from a microbore teflon tube, which is tricky.

A magnifying glass is used for precise positioning of the syringe plunger to increase the accuracy of filling.

The syringe needle is filled with sample by a sandwich technique in the following order: first aspiration of 0.2 μl water, then aspiration of 0.05 μl sample (in $CHCl_3$:MeOH, 1:1 v:v) followed by aspiration of 0.01 μl air, and finally aspiration of 0.09 μl water. The sandwich technique for filling the needle, which creates an air/water cushion on top of the sample, prevents direct contact between the sample and the bubble's air-water interface in the absence of active injection. Thus it provides as much time as required for careful positioning of the needle tip without risking uncontrolled spreading of sample. Although the sandwich technique cannot prevent part of the MeOH used in the sample solution from partitioning inside the needle into the contacting water cushion, none of our experiments appear to have been affected by $CHCl_3$:MeOH.

Once the syringe plunger is positioned and the syringe needle is filled, the needle is introduced into the sample chamber through the polyethylene tube located in the center of the gasket and advanced under video control (side view) until the tip makes contact with the bubble. Under video control (top view), the alignment of the needle tip and the opening of the polyethylene tube, one above the other, is checked. If the two are not aligned, the position of the tip is optimized by gentle tilting of the syringe body. Next, the complete contents of the needle are slowly (~10 s) pushed out. The shape of the bubble must be carefully observed to detect the onset of sample spreading, indicated by flattening of the bubble. Flattening will eventually cause the bubble to detach from the needle tip, thereby making spreading of film unreliable. To avoid detachment, one follows the bubble with the needle, while continuing the injection. After the injection is completed, the syringe is removed slowly to avoid perturbing the film during detachment of the needle tip. Then stirring is started (100 rpm for 60 min) to increase desorption of solvent from the air-water interface into the subphase. Solvent that has dissolved in the subphase is then washed out by perfusion of the sample chamber with 7 ml of subphase buffer (~10-fold exchange of subphase volume by gravity flow) over a period of 30 min. Throughout perfusion the subphase is stirred, and the temperature inside the sample chamber is kept constant at 37°C.

Method evaluation

We evaluated the technique by investigating the reliability, precision, and accuracy with which a film can be formed, by assessing the effect of the solvent used for film formation on surface tension, and by comparing the surface activity of hydrophobic surfactant protein-phospholipid film formed by spreading with that of film formed by adsorption during rapid cyclic area changes.

Reliablity, precision, and accuracy

To determine the reliability of the technique, the number of times we could successfully spread film was compared with the number of times we tried.

To assess the precision and the accuracy of the technique, various amounts of DPPC (0.16–0.04 μg dissolved in 0.05 μl $CHCl_3$:MeOH, 1:1 v:v) were spread in series along the bubble's air-water interface at spreading pressures of >45 mN/m (bubble area before spreading of film, 0.5 cm^2) and <45 mN/m (bubble area before spreading of film, 1.0 cm^2). After 60 min of stirring, the sample chamber was perfused with subphase buffer as described above (unless otherwise stated). Next a compression surface tension/area isotherm was inscribed by raising the cuvette pressure from 1.0 to 4.0 ata within 3 s. The area per molecule at a given surface tension was calculated from the amount of DPPC that was spread by measuring the phosphorus content in the DPPC stock solution according to the method of Bartlett (1959). Precision is expressed as the maximum difference in area per molecule between compression surface tension-area isotherms spread at identical conditions. Accuracy is expressed by comparing the area per molecule between compression surface tension-area isotherms inscribed in this CBS with that of isotherms obtained in another CBS (Schürch et al., 1989) and in a Wilhelmy balance (Goerke and Clements, 1986).

Effect of solvent on surface tension

Because a solvent must be used to enable the surfactant to spread along the bubble's air-water interface, it is important that the solvent not contain contaminants that might impair the surface activity of the film. The effect of solvent on the surface tension of subphase buffer was assessed by spreading 0.05-μl aliquots of solvent ($CHCl_3$:MeOH, 1:1 v:v) at the air-water interface of the bubble. After 60 min of subphase stirring (100 rpm; no perfusion), the cuvette pressure was raised to 2.8 ata, and the bubble was recorded on videotape for calculation of surface tension and area.

Because solvent retained in the system after spreading of film can destroy the surface activity of a surfactant film, it is important to eliminate solvent after spreading. To assess the effect of solvent on the surface tension of a preformed phospholipid film and to determine whether it can be washed out by perfusion of the sample chamber, multilamellar vesicles were formed by hydrating a dried lipid sample (DPPC:POPG, 80:20 mol%) in 1.5-ml subphase buffer at 50°C with a vortexer. Then small unilamellar vesicles were prepared from the multilamellar vesicles by sonication at 50°C with a sonifier (Sonopuls HD 70; Bandelin, Berlin, Germany) equipped with a microtip 0.3 cm in diameter (MS 73), for 2 min at 25 W. Next the cuvette was filled with small unilamellar vesicles, and a bubble was formed by injection of air (29 μl). The lipid film was formed from the stirred suspension of small unilamellar vesicles by adsorption over a period of 60 min. The sample chamber was then perfused with subphase buffer as described above to wash out vesicles. Then 0.05 μl of solvent ($CHCl_3$:MeOH, 1:1 v:v) was injected into the air-water interface, and the bubble was recorded for calculation of surface tension and area. Sixty minutes later the sample chamber was perfused as described above to wash out solvent, and surface tension was measured again.

Comparison of surface activity of film formed by spreading and by adsorption during rapid cyclic area changes

To be able to apply this spreading technique to comparative studies of surface activity of spread film and adsorbed film, we compared the surface activity of film formed by both techniques.

Sample preparation. Before reconstitution of hydrophobic surfactant protein-phospholipid mixtures, concentrations and content of the components were determined. The concentration of both DPPC (10.8 mg/ml) and POPG (9.7 mg/ml) stock solutions ($CHCl_3$:MeOH, 1:1 v:v) was determined according to the method of Bartlett (1959). The concentration of pig surfactant protein B (SP-B) (0.088 mg/ml) and pig surfactant protein C (SP-C) (0.087 mg/ml) stock solutions ($CHCl_3$:MeOH, 1:1 v:v), isolated according to the method of Oosterlaken-Dijksterhuis et al. (1991), was measured by fluorescamine assay according to the method of Böhlen et al. (1973) and by quantitative amino acid analysis. The phospholipid content in the SP-B stock solution was unmeasurable; in the SP-C stock solution it was 0.22 nmol phospholipid/μg SP-C when measured according to the method of Bartlett (1959).

For spread film experiments, hydrophobic surfactant protein-phospholipid mixtures were reconstituted as follows. Aliquots (9 μl) were transferred from the DPPC:POPG stock solution (80:20 mol%) with a glass syringe (801; Hamilton) into pointed glass vials (100 μl; Roth, Karlsruhe, Germany) and dried under a stream of N_2 gas at 37°C. Then aliquots (174 μl) from the SP-B:SP-C stock solution (10:90 mol%) were added (825; Hamilton). In controls (DPPC:POPG 80:20 mol%), 174 μl of solvent ($CHCl_3$:MeOH, 1:1; v:v) without SP-B:SP-C was added. After gentle mixing on a vortexer, the mixture of DPPC:POPG:SP-B:SP-C or DPPC:POPG was dried again under N_2 gas at 37°C and stored at −80°C. Before formation of the initial film by spreading, dried samples were dissolved in

25 μl solvent ($CHCl_3$:MeOH, 1:1 v:v). The wall of the pointed glass vial was rinsed carefully after the dried samples were dissolved in solvent, and the sample was mixed by repeated vortexing and aspiration into a glass syringe (805; Hamilton). The calculated final molar composition of DPPC:POPG:SP-B:SP-C in sample solutions prepared for spreading of film was 78.25:19.55:0.20:2.00 mol%. The final molar composition of DPPC:POPG in controls was 80:20 mol%.

The amount of material spread was standardized to 0.15 μg DPPC (which is 11% more DPPC than the interface can hold at a surface tension of 25 mN/m) plus associated amounts of POPG with or without SP-B and SP-C. Thus film was always formed at conditions of surface excess, which leaves the composition of the interfacial monolayer uncertain.

For adsorbed film experiments, hydrophobic surfactant protein-phospholipid mixtures were reconstituted as follows. Aliquots (179 μl) from the mixed solution of DPPC:POPG (80:20 mol%) were transferred with a glass syringe (825; Hamilton) into 10.0-ml conical glass tubes and dried under a stream of N_2 gas at 37°C. Next 3473-μl aliquots from the mixed SP-B:SP-C solution were added to the dried lipids. In controls (DPPC:POPG, 80:20 mol%), 3473 μl of solvent without SP-B:SP-C was added to the dried lipids. After gentle mixing on a vortexer, the mixture of DPPC:POPG:SP-B:SP-C or DPPC:POPG was dried again under N_2 gas at 37°C and stored at −80°C. Before formation of the initial film by adsorption, multilamellar vesicles were formed by hydrating a dried sample in 1.5 ml of buffer solution (as described above). Residual material stuck to the glass wall of the conical glass tube was rinsed off with a pipettor (1-ml tip). Next, small unilamellar vesicles were prepared from multilamellar vesicles (as described above). The calculated final molar composition of DPPC:POPG:SP-B:SP-C in small unilamellar vesicles prepared for adsorption of film was 78.25:19.55:0.20:2.00 mol%. The final molar composition of DPPC:POPG in controls was 80:20 mol%. Experiments were performed only at DPPC:POPG:SP-B:SP-C of 78.25:19.55:0.20:2.00 mol% because of the large amounts of SP-B and SP-C required.

Because components of the surfactant film are thought to be repeatedly replaced during cyclic area changes, small unilamellar vesicles (without proteins) were injected into the subphase before cycling of the film to act as a source of material for film formation. In each experiment, small unilamellar vesicles were freshly prepared by sonication of multilamellar vesicles (DPPC:POPG, 80:20 mol%; 23.3 mg DPPC/ml) at 50°C as described above. Before injection into the subphase, the suspension was mixed on a vortexer. A 30-μl sample was withdrawn with a glass syringe (805, needle gauge 22S; Hamilton) and slowly injected into the stirred subphase (final subphase concentration 1.0 mg DPPC/ml).

Experimental protocol. For spread film experiments, first a phospholipid film with or without proteins was spread at the bubble's air-water interface as described above. Next stirring was started, and the subphase was stirred at 100 rpm for 60 min to enhance desorption of solvent. After the sample chamber was perfused with subphase buffer, freshly prepared small unilamellar vesicles (without proteins) were injected into the stirred subphase to provide a source of substrate for film formation, and stirring was continued for another 15 min. Then the bubble's area was expanded by sudden lowering of the cuvette pressure to 0.5 ata for 10 s to study adsorption. The bubble was then cycled five times (6 cycles/min) between 2.8 and 0.5 ata to measure the surface activity of film during dynamic cyclic area changes. At the end of the fifth compression, the cuvette pressure was kept constant for a period of 5 min (2.8 ata) to determine film stability after cyclic area changes.

For adsorbed film experiments, a sample of ~0.9 ml was withdrawn from the sample suspension with a Pasteur pipette and loaded into the cuvette. The cuvette was then mounted in the cuvette holder, sealed, inverted, and placed in the plexiglas enclosure. A bubble was formed by injection of air (29 μl) at 37°C according to the method of Putz et al. (1994a), and a film was allowed to form for 60 min at the bubble's air-water interface by adsorption from the stirred suspension of small unilamellar vesicles with or without (control) proteins. Next the sample chamber was perfused to wash out the small unilamellar vesicles. Expansion of the bubble's area and all subsequent steps were the same as described for spread film.

Surface activity was assessed by measuring the adsorption speed, the minimum and maximum surface tension, and the compressibility and the stability of the film. Adsorption speed is expressed as the surface tension of film reached 1 and 10 s after sudden bubble expansion. Minimum surface tension was defined as the surface tension of film reached during compression before onset of film collapse, where film collapse was defined as a decrease in bubble diameter at constant bubble height. Maximum surface tension was defined as the highest surface tension of film reached during expansion. Film compressibility (C) is expressed at a surface tension (γ) of 15 mN/m as $C = (1/A)\times(dA/d\gamma)$, where A is the area of the bubble. $dA/d\gamma$ was obtained from fourth-degree least-squares polynomial fits (KaleidaGraph, version 3.0.4; Synergy Software, Reading, PA) to dynamic compression isotherms. Film stability was determined as $d\gamma/dt$ by measuring surface tension at constant cuvette pressure (2.8 ata) for 5 min. This determination was made at the end of the fifth compression, if the surface tension was less than 5 mN/m. $d\gamma/dt$ was obtained from linear fits to a data set of surface tensions measured at four time points (0, 1, 3, and 5 min). This analysis overestimates the stability of film because it does not account for the area change of the bubble caused by desorption of gas out of the bubble and into the subphase. The surface-associated phase was defined as the phase when particulate matter was firmly associated with the bubble's air-water interface. This phase was seen on the television monitor to appear and disappear during cyclic area changes resulting from dynamic bubble compression and expansion and was seen during static bubble compression (film stability).

Quality assurance and quality control of data obtained

To ensure that phospholipid-hydrophobic surfactant protein or phospholipid film was spread at a clean air-water interface, the bubble was always compressed rapidly (~54% area reduction) before spreading of film and surface tension were measured. Only bubbles with a surface tension equal to or greater than 68 mN/m at minimum bubble area were accepted for spreading. In adsorbed film experiments, this test could not be performed because the bubble was formed in either a phospholipid-hydrophobic surfactant protein or phospholipid suspension. To ensure that the bubble was a symmetrical figure of revolution, it was continuously viewed from the top. At the end of the experiment, the bubble was recorded separately for measurements of side-to-side and front-to-back diameters during both static (at highest cuvette pressure) and dynamic compression. During recording, the contrast between the bubble's contour and the gasket was increased by additional illumination of the sample chamber with a flashlight. Experiments with bubbles with a difference between side-to-side and front-to-back diameters greater than 2% were excluded from analysis.

To eliminate the possibility that the true surface activity of phospholipid-hydrophobic surfactant protein film was masked by a pH that is too low (Qanbar and Possmayer, 1995), pH was checked in a series of experiments at the end of the experimental protocol with pH paper (9543, color scale graduated in 0.3 pH units; Merck, Darmstadt, Germany). To exclude the possibility that phospholipids were degraded by sonication, the temperature was measured before and after 2 min of sonication in suspensions of multilamellar vesicles with and without proteins used for film formation by adsorption. In addition, aliquots were extracted after sonication for thin-layer chromatography (TLC) according to the method of Bligh and Dyer (1959), separated on silica gel plates according to the method of Touchstone et al. (1980), and visualized by spraying. Spots were wetted, scraped off the glass plate, and extracted according to the method of Bligh and Dyer (1959), and amounts of phospholipid per spot were determined in triplicate according to the method of Bartlett (1959).

Statistical analysis

Spread and adsorbed film experiments were performed in random order. Data are reported as means ± SE.

RESULTS

Method evaluation

Reliability, precision, and accuracy

The spreading technique reliably spread film along the bubble's air-water interface. In all 44 experiments that we tried, film was spread successfully. The precision of the technique was high when film was formed at a spreading pressure greater than 45 mN/m (Table 1). It was low, however, when the spreading pressure was less than 45 mN/m. The accuracy of rapid compression surface tension-area isotherms was within that of previously published surface tension-area compression isotherms for a spreading pressure less than 45 mN/m (Fig. 2).

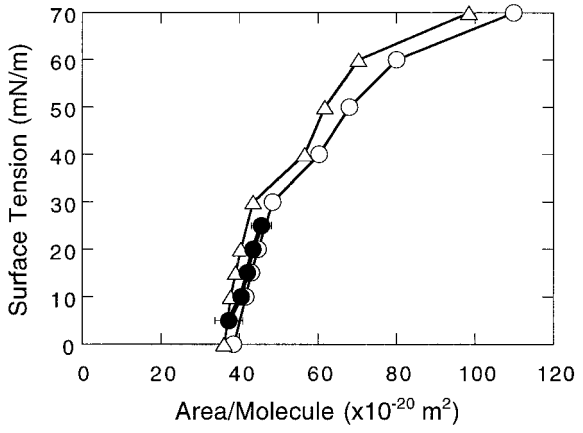

FIGURE 2 Comparison of surface tension-area compression isotherms for spread dipalmitoylphosphatidylcholine film at 37°C in three different systems. ●, Rapid compression isotherm for dipalmitoylphosphatidylcholine (0.16 and 0.12 μg) spread along bubble's air-water interface of 0.5 cm^2, as described in Materials and Methods. Data are means ± SE for six experiments. SE bars are partly obscured by symbols. △, Quasistatic compression isotherm for dipalmitoylphosphatidylcholine inscribed in another captive-bubble surfactometer (data taken from Schurch et al., 1989). ○, Compression isotherm for dipalmitoylphosphatidylcholine inscribed in a Wilhelmy balance (data taken from Goerke and Clements, 1986).

Effect of solvent on surface tension

Aliquots of 0.05 μl of solvent spread along the air-water interface of a bubble without a lipid film did not change surface tension (Table 2). In contrast, aliquots of 0.05 μl of solvent spread at the air-water interface of a bubble containing a lipid film preformed by adsorption from a suspension of small unilamellar vesicles lowered surface tension by 10% (Table 2). The effect was reversible: upon stirring for 60 min and subsequent perfusion of the sample chamber, surface tension returned to the initial value. Larger aliquots of solvent always lowered surface tension when spread along the air-water interface of a bubble without a lipid film (data not shown). The compressiblity of spread DPPC film in the presence of a washing step was 0.009 ± 0.001 (Table 3).

Comparison of surface activity of film formed by spreading and by adsorption during rapid cyclic area changes

In the first second after a sudden bubble expansion of comparable area increase, surface tension in spread film with proteins was almost as low as that in adsorbed film with proteins (40.7 ± 1.3 versus 34.3 ± 1.2 mN/m) (Fig. 3) and was equally low by 10 s (25.5 ± 0.5 versus 24.0 ± 0.4 mN/m). Results were similar for film without proteins. In the first second after a sudden bubble expansion of comparable area increase, surface tension in spread film without proteins was almost as low as that for adsorbed film without

TABLE 1 Precision of the spreading technique for DPPC film during rapid bubble compression at 37°C at various surface tensions

Surface tension (mN/m)	Difference (Å^2/molecule)	
	>45 mN/m	<45 mN/m
25	—	18.5
20	2.5	18.5
15	2.5	19.0
10	3.0	19.0
5	2.0	20.0

Precision is expressed as the maximum difference in area per molecule between rapid compression surface tension/area isotherms for three experiments in which DPPC film was spread at identical conditions. >45 mN/m, spreading pressure >45 mN/m, which was obtained by spreading 0.16 or 0.12 μg DPPC (dissolved in 0.05 μl $CHCl_3$:MeOH, 1:1 v:v) along the air-water interface of a 0.5 cm^2 bubble. <45 mN/m, spreading pressure <45 mN/m, which was obtained by spreading 0.08 or 0.04 μg DPPC (dissolved in 0.05 μl $CHCl_3$:MeOH, 1:1 v:v) along the air-water interface of a 0.5 cm^2 bubble and 0.16 or 0.12 μg DPPC spread along the interface of a 1.0 cm^2 bubble.

TABLE 2 Effect of solvent on surface tension when spread along the air-water interface of a bubble with and without a phospholipid film at 37°C

Intervention	Surface tension (mN/m)	
	Without film (n = 4)	With film (n = 5)
Before spreading of solvent	70.2 ± 0.4	48.4 ± 2.6
Upon rapid bubble compression (area reduction 53%)	70.0 ± 0.4	ND
After spreading of solvent	69.5 ± 0.5	43.1 ± 2.9
After stirring of subphase buffer for 60 min and perfusion of sample chamber	69.9 ± 0.4	48.1 ± 2.6
Upon rapid bubble compression (area reduction 54%)	69.9 ± 0.6	ND

Solvent: 0.05 μl $CHCl_3$:MeOH (1:1 v:v). Without film: A bubble was formed in subphase buffer (140 mM NaCl, 10 mM HEPES, 0.5 mM EDTA, 2.5 mM $CaCl_2$, pH 6.9) without a phospholipid film at 37°C. With film: A phospholipid film was formed by adsorption to the bubble's air-water interface from a stirred suspension of small unilamellar vesicles (DPPC:POPG, 80:20 mol%) in subphase buffer. ND, Not determined. Data are means ± SE.

TABLE 3 Compressibility of spread and adsorbed phospholipid-hydrophobic lung surfactant protein and phospholipid film upon rapid bubble compression at 37°C

Ratio of film components* (mol%)	Film compressibility at 15 mN/m (m/mN)					
	Spread film			Adsorbed film		
	1st comp	3rd comp	5th comp	1st comp	3rd comp	5th comp
78.25:19.55:0.20:2.00	0.008 ± 0.001 (8/8)[#]	0.008 ± 0.001 (8/8)	0.008 ± 0.001 (8/8)	0.019 ± 0.003 (8/10)	0.010 ± 0.002 (10/10)	0.008 ± 0.001 (10/10)
80:20:0:0	0.017 ± 0.002 (10/10)	0.013 ± 0.002 (10/10)	0.013 ± 0.002 (10/10)	(0/10)	0.015 (1/10)	0.012 (1/10)
100:0:0:0[§]	0.009 ± 0.001 (9/9)	ND	ND	0.009 ± 0.001 (14/14)[¶]	ND	ND

*DPPC:POPG:SP-B:SP-C. 1st, 3rd, and 5th comp, 1st, 3rd, and 5th rapid compression of film. Film compressibility (C) is expressed as $C = (1/A) \times (dA/d\gamma)$ at a surface tension of 15 mN/m.

[#]Numbers in parentheses = the number of experiments analyzed/number of experiments performed. Experiments were analyzed only if the film reached a minimum surface tension of <15 mN/m at minimum bubble area.

[§]DPPC (0.16 or 0.12 μg dissolved in 0.05 μl $CHCl_3$:MeOH, 1:1 v:v) spread along the air-water interface of a 0.5 cm^2 bubble (spreading pressure >45 mN/m) or a 1.0 cm^2 bubble (spreading pressure <45 mN/m) and rapidly compressed after perfusion of the sample chamber. ND, not determined.

[¶]DPPC film was formed by adsorption from a 1 mg/ml suspension in subphase buffer at 41°C over a period of 30 min and compressed slowly at 37°C under quasistatic conditions. Data are means ± SE.

proteins (68.7 ± 0.9 versus 64.1 ± 1.4 mN/m) and almost equally low at 10 s (65.6 ± 1.6 versus 61.3 ± 1.5 mN/m).

The minimum surface tension reached by spread film with proteins during cyclic area changes was as low as that for adsorbed film with proteins (Fig. 4 and 5). However, the maximum surface tension for spread film with proteins was higher. For spread film without proteins, the minimum surface tension was lower during cyclic area changes than for adsorbed film without proteins (Figs. 4 and 5). The maximum surface tension for spread film without proteins

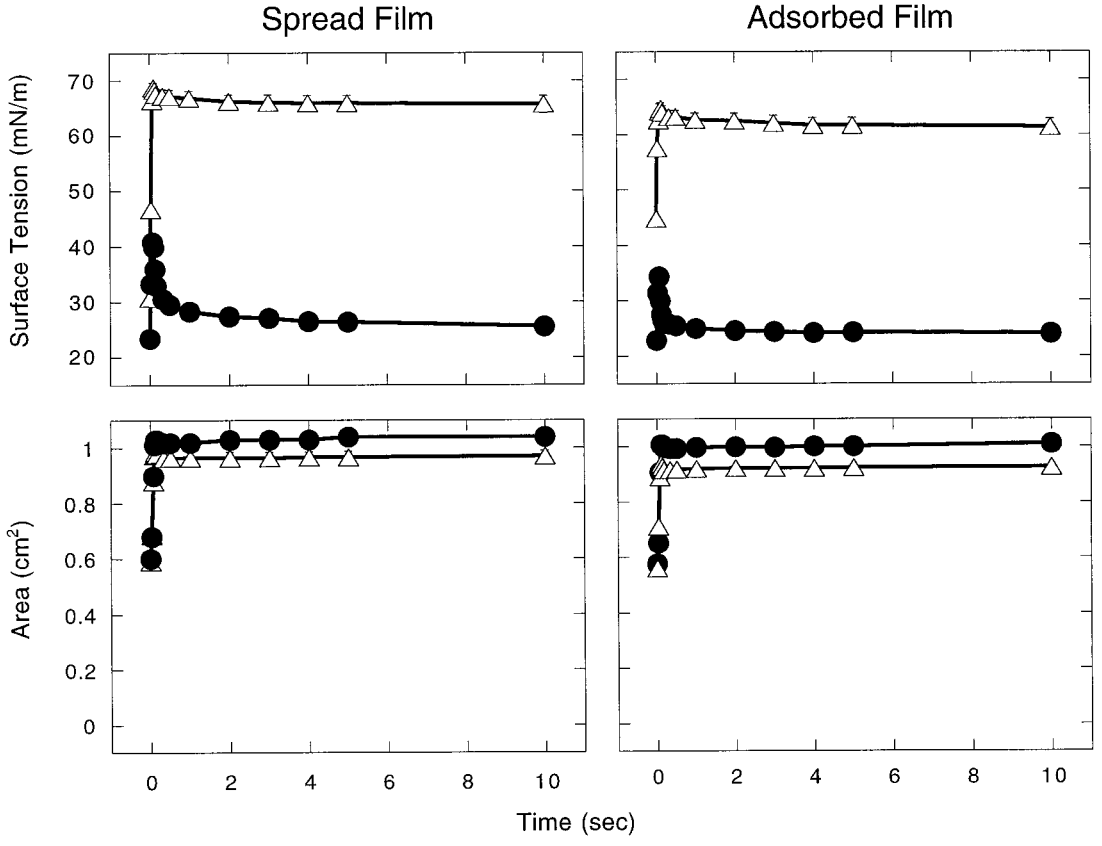

FIGURE 3 Adsorption kinetics for spread and adsorbed phospholipid-hydrophobic lung surfactant protein and phospholipid film after a rapid decrease in cuvette pressure to expand the bubble. ●, Film with proteins. △, Film without proteins. Data are means ± SE for 8–10 experiments. SE bars are partly obscured by symbols.

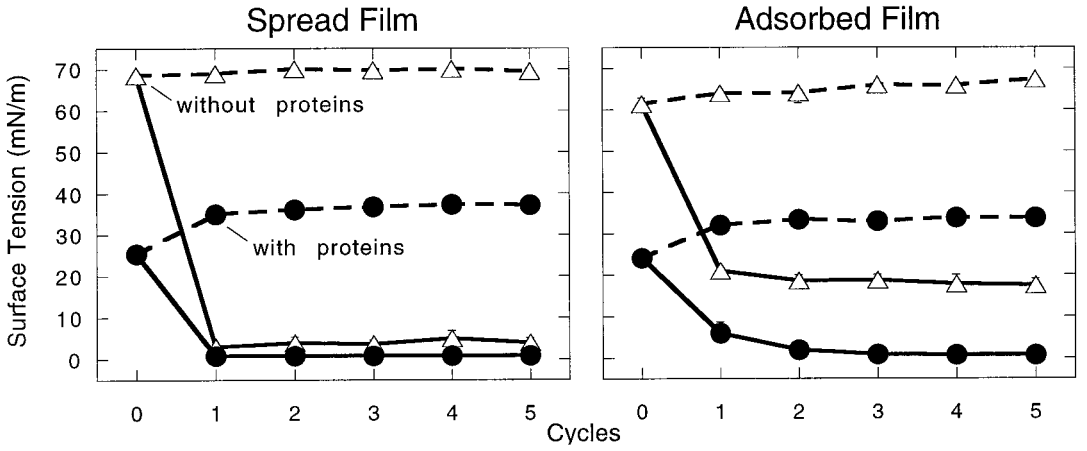

FIGURE 4 Minimum (——) and maximum surface tension (– – –) of spread and adsorbed phospholipid-hydrophobic lung surfactant protein and phospholipid film during cyclic area changes. Data for cycle 10 (not shown) were similar to data shown for cycle 5. Symbols are the same as those in Fig. 3. Data are means ± SE for 8–10 experiments. SE bars are partly obscured by symbols.

was higher during the first three cycles but equally high thereafter.

The shape of the compression-expansion isotherms recorded during rapid cyclic area changes suggests that there was ongoing respreading of film components during bubble expansion in the presence of surfactant proteins for both spread and adsorbed film (Fig. 5), as indicated by the maximum surface tension, which stayed constantly low upon repeated expansion.

On the first compression, the compressibility of spread film with proteins was lower than that of adsorbed film with proteins (Table 3 and Fig. 5, *A* and *B*). This finding is in accordance with the squeeze-out plateaus seen for adsorbed film with proteins (Fig. 5 *B*). However, on the third through fifth compressions, no differences were found. The compressibility of spread film without proteins was higher than that of spread film with proteins (Table 3 and Fig. 5, *A* and *C*). For adsorbed film without proteins the compressibility could be determined in only one out of 10 experiments and only on the third and fifth compressions. It was the same as that of spread film without proteins.

The stability of spread film with proteins was similar to that of adsorbed film with proteins (0.006 ± 0.003 and 0.003 ± 0.004 (mN/m)/min; $n = 8$ and 10 experiments). No comparisons were made for spread and adsorbed film without proteins because film formed by adsorption reached a surface tension of <5 mN/m in only one out of 10 experiments.

For spread film with proteins, a surface-associated phase, defined as particulate matter firmly associated with the bubble's air-water interface, was seen during compression in only one of nine experiments. In contrast, such a surface-associated phase was always seen in adsorbed film with proteins. It was never seen in spread or adsorbed film without proteins.

Quality assurance and quality control of data obtained

Covering the rubber gasket with agarose prevented the release of surface-active contaminants. No experiment had to be rejected because the initial surface tension was less than 68 mN/m on bubble compression (surface tension of bubbles in buffer before spreading of film was 70.0 ± 0.1 mN/m at 1.0 ata and 70.0 ± 0.1 mN/m at 2.8 ata; area reduction 51%; $n = 34$ experiments).

The bubble remained a symmetrical figure of revolution not only during static but also during dynamic compression. From a total of 117 frames of phospholipid-hydrophobic surfactant protein and phospholipid film experiments recorded during both static and dynamic compressions, only three frames differed by more than 2% between side-to-side and front-to-back diameters. The ratio of side-to-side to front-to-back diameters of bubbles from spread film experiments was 1.000 ± 0.001 ($n = 48$ frames). For adsorbed film experiments it was also 1.000 ± 0.001 ($n = 69$ frames).

The pH of the subphase buffer measured at the end of the experimental protocol was always within the range of 6.8–7.1 pH units for both spread film experiments ($n = 15$ experiments) and adsorbed film experiments ($n = 9$ experiments).

The temperature measured in the suspension of small unilamellar vesicles used for adsorption experiments (with and without proteins) and subphase injection was 48.9 ± 0.2°C before sonication and 48.4 ± 0.5°C after 2 min of sonication ($n = 28$ experiments). LPC and PA were detectable after sonication in suspensions of small unilamellar vesicles with proteins by TLC (LPC was 12 ± 1%; a PA spot was visible in seven of 12 experiments). In the only experiment available before and after sonication for analysis of lipid degradation by TLC, LPC and PA were detectable both before and after sonication (LPC was 6% and 8% of total phosphorus; PA was visible both times). LPC was also detectable after sonication in small unilamellar vesicles without proteins (6 ± 1%; $n = 3$ experiments), whereas PA was not.

DISCUSSION

We have developed a spreading technique that allows routine formation of film by spreading of small amounts of

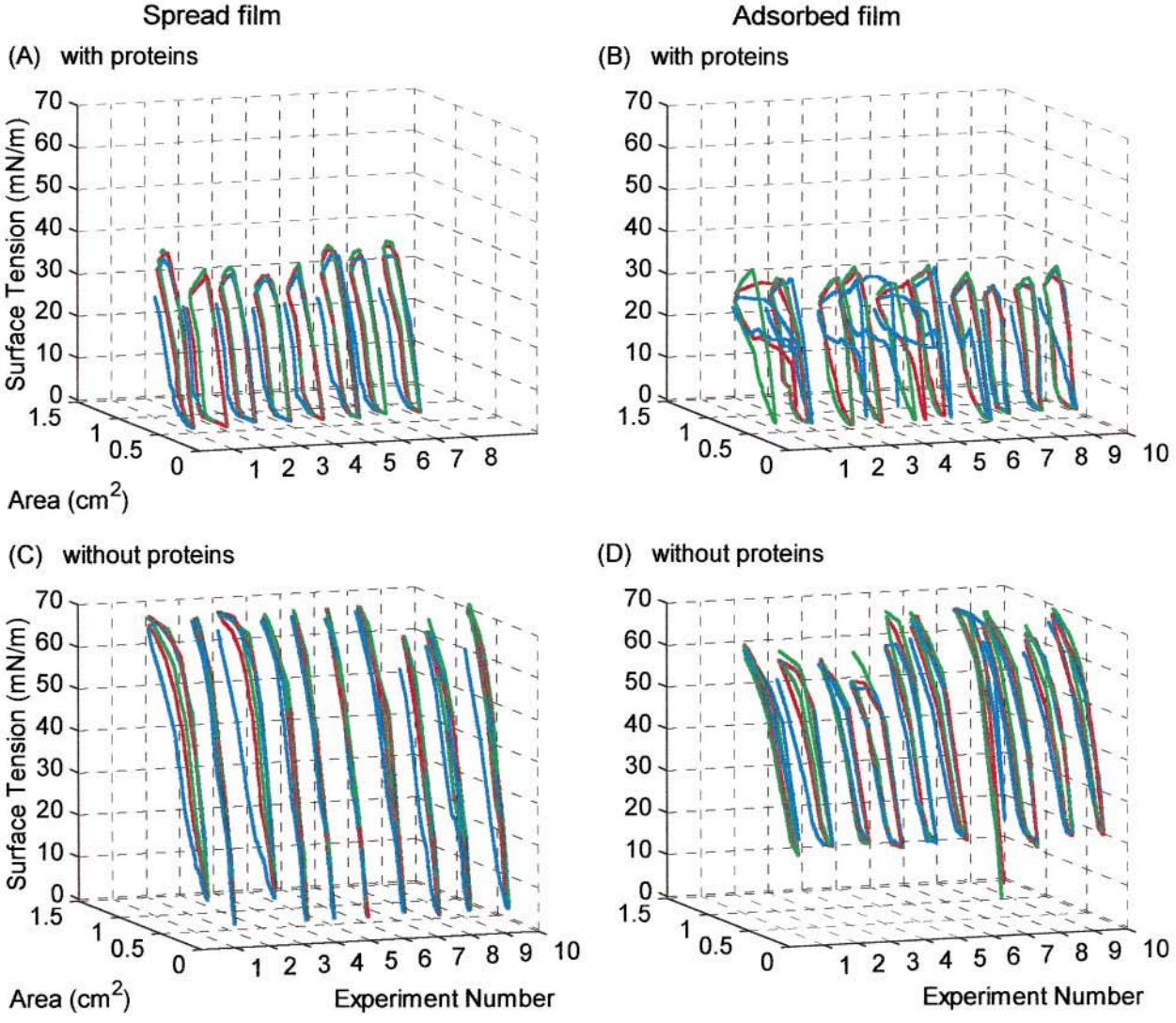

FIGURE 5 Surface tension-area compression-expansion isotherms for spread and adsorbed phospholipid-hydrophobic lung surfactant protein and phospholipid film during cyclic area changes (6 cycles/min). (*A* and *C*) Film formed by spreading with and without proteins. (*B* and *D*) Film formed by adsorption with and without proteins. Blue, red, and green, first, second, and third compression-expansion isotherms. Individual data sets are shown for 8–10 experiments.

surfactant components at the air-water interface of an air bubble in a CBS. Our evaluation of this technique shows that it is reliable, precise, and accurate. Specifically, of 44 consecutive attempts to spread a film along the bubble's air-water interface, all 44 attempts were successful. In addition, film can be formed with high precision, and rapid compression surface tension-area isotherms can be inscribed with high accuracy if spreading pressure is greater than 45 mN/m (Table 1 and Fig. 2).

Our application of this technique to a comparative study of spread and adsorbed film shows that the biophysical activity of film formed by spreading is similar to that of film formed by adsorption. The differences in surface activity observed are very small (Figs. 3–5 and Table 3). Specifically, we found that the surface activity is slightly lower for spread film with proteins than for adsorbed film with proteins and slightly higher for spread film without proteins than for adsorbed film without proteins.

For film with proteins, several reasons could explain the small differences in surface activity that we observed. First, for spread film with proteins we could practically never detect a surface-associated phase, whereas for adsorbed film with proteins we always could. As was recently shown for adsorbed film, a surface-associated phase can act as a reservoir, from which surplus material is recruited into the surface-active film during an increase in surface area (Schürch et al., 1995). Thus it is possible that the differences observed in the speed of film formation (e.g., surface tension reached 1 and 10 s after a sudden bubble expansion and maximum surface tension reached during cyclic area changes) can be attributed at least in part to differences in reservoir size.

Second, these differences in surface activity may be attributed to differences in composition of the film. For spread film with proteins, we calculated the amount of material spread along the bubble's air-water interface (0.5 cm^2) as being threefold more than the amount required for complete coverage of the surface at a surface tension of 35 mN/m with a monomolecular film. Spreading of excess material in conjunction with the high spreading pressure of ~45 mN/m used in this study could have induced surface sorting with preferential squeeze-out of low-compressibility components such as SP-B, which was previously shown to be squeezed out during film compression at a surface tension of ~30 mN/m (Taneva and Keough, 1994), and/or POPG (Yu and Possmayer, 1990). As a consequence, the film could have become enriched in low-compressibility components. For this reason, the compressibility of film formed by spreading but not by adsorption would have been as low on the first compression as that of DPPC, as in fact was found (Table 3). In contrast to film formed by spreading, film formed by adsorption regularly showed large squeeze-out plateaus on the first compression (Fig. 5 *B*). Separation of phospholipids used for film formation by TLC and analysis of phosphorus content revealed that some LPC was generated by sonication. Both LPC and PA, which is also generated during degradation, are surface-active components capable of destroying the surface activity of a surfactant film (Holm et al., 1991; Enhorning et al., 1992). Therefore it is likely that LPC and PA were part of the film initially formed by adsorption, were squeezed out during bubble compression, and did not readsorb during bubble expansion until finally film compressibility (Table 3) and the extent of observed overcompression (data not shown) were the same as in film with proteins formed by spreading. Thus it seems likely that differences in the composition of the film due to differences in the experimental protocol rather than structural alterations of the lipid and/or protein components caused by spreading contributed to the differences in surface activity observed.

Third, differences in surface activity could have been caused by lipid degradation, which can occur during preparation of small unilamellar vesicles (Szoka and Papahadjopoulos, 1980). TLC and phosphorus analysis performed on a single sample showed that it contained more LPC after sonication. Sonication, if applied extensively, can cause lipid and protein degradation either by heat or by pulse waves. We found that the temperature measured in samples during sonication remained constant. This constant temperature would suggest that the pulse waves generated during sonication were responsible for the lipid degradation observed. Whether it resulted in additional damage to the proteins was not further investigated. It was recently shown that substantial amounts of LPC are also rapidly generated upon incubation of phospholipid film with SP-C in $CHCl_3$:MeOH:0.1 N HCl (Qanbar and Possmayer, 1995). We do not know whether some HCl left from protein purification also contributed to lipid degradation. We did not address this issue further.

For film without proteins, a comparison of surface activity of spread film with that of adsorbed film is difficult because, in contrast to spread film, adsorbed film reached low surface tensions only occasionally (Figs. 4 and 5). Differences in the experimental approach (e.g., surface tension before a sudden increase in bubble area was lower for spread film than for adsorbed film) most likely explain this finding. Recently (Nag et al., 1996) found that spread and adsorbed monolayers of DPPC and SP-C have analogous properties when formed at low surface pressure (<1 mN/m) before film compression. Our results, performed in a different system and at different conditions, confirm this finding. Furthermore, they demonstrate that spread film can adsorb fast, almost as fast as adsorbed film that was formed at a subphase concentration, which is known to result in rapid film formation. Our results further suggest that larger quantities of material are closely associated with the surface film and readily fill in empty space in the air-water interface when this interface is opened up by rapid bubble expansion.

Our technique has three main advantages. First, the technique allows spreading of film along the air-water interface of an air bubble with great ease and without the need for special equipment. This ease was made possible by reconstructing the CBS (Fig. 1) and by refining the technique of film spreading. The major factors of the reconstruction that contribute to the ease of use are mounting the plexiglas enclosure on a split beam, which provides easy access to the bubble's air-water interface with a syringe needle, and mounting a second video camera on top of the plexiglas enclosure, which aids in positioning the needle tip at the bubble's apex. The major factor of refining the technique of film spreading that contributes to the ease of use is the conventional positive displacement-type glass syringe with a blunt tip, which simplifies transfer of sample from the test tube to the bubble's air-water interface and spreading of film.

The second main advantage of this technique is that it requires only small amounts of material (microgram range) for tests of the biophysical activity of surfactant in a leakproof surfactometer. This is important in situations where detailed information about the surface activity of a specimen (for example, from a bronchoalveolar lavage sample or from an expression system) is crucial, but the amount available for analysis is limited (E. J. A. Veldhuizen et al., manuscript submitted for publication).

The third main advantage of this technique is that it can be used for mechanistic studies of surfactant protein-phospholipid interactions of spread film or comparative studies of spread and adsorbed film.

In addition to the ease of use, the small amount of surfactant required, and the applicability to mechanistic and comparative studies, this spreading technique has three other advantages. First, in the original pressure-driven CBS (Putz et al., 1994a) the release of surface-active agents from the gasket was a problem. In our new system, the bubble's air-water interface is now kept free of surface-active agents that could contaminate it by covering the gasket with a layer

of purified agarose. Surface contamination, as indicated by a drop in surface tension during rapid compression of the bubble in water (~50% area reduction), is no longer found.

Another advantage is that this set-up allows checking of the bubble's axisymmetry during dynamic cyclic area changes. This has become possible with the second video camera, which is also helpful for centering the bubble and which replaces the front surface-coated glass mirror originally recommended by Putz et al. (1994a). Checking the bubble's axisymmetry is necessary because the flow of liquid into and out of the sample chamber during dynamic cyclic area changes is rapid. Thus deviation of the bubble's shape from axisymmetry caused by deformation (jet of liquid) and/or displacement of the bubble is always possible. Any deviation from axisymmetry leads to the calculation of erroneous results for surface tension and bubble area. Therefore, axisymmetry is a prerequisite for accurate surface tension and bubble area measurements and reconstruction of surface tension-area isotherms inscribed in a CBS (Schoel et al., 1994; Holm et al., 1991). Analysis of the bubble's shape in a series of experiments from the top during dynamic cyclic area changes revealed that three out of 117 frames were distorted. They were from a single experiment in which there was a problem with the pressure device. We have not seen this problem in numerous other experiments performed after that series of measurements was finished.

Finally, it should be mentioned that the spreading technique does not affect the pH of the sample buffer. It was recently shown that the surface activity of phospholipid film containing SP-C is markedly improved when the pH is low (Qanbar and Possmayer, 1995). This improvement was attributed to alterations in net charge and charge distribution, which in turn seem to affect lipid-lipid, lipid-protein, and lipid-protein-water interactions. We found that the pH of the subphase did not drop to <6.8 pH at any time during the course of the experiment, indicating that the spreading technique does not affect the biophysical activity of a surfactant film.

Our technique has two minor limitations. One limitation is the solvent required for spreading of film. The volume of solvent used for formation of film decreased the surface tension when injected into the air-water interface of a bubble containing a lipid film formed by adsorption from a suspension of small unilamellar vesicles (Table 2). It did not decrease surface tension when spread at the air-water interface of a bubble in buffer. This result suggests that solvent (presumably $CHCl_3$) is retained in both film and bubble after spreading. Although the amount of solvent retained did not impair the compressiblity of the DPPC film in the absence of a washing step (data not shown), we recommend, in accordance with Schürch et al. (1989), exchanging the subphase before the film is compressed. Exchanging the subphase will ensure that any solvent that has dissipated into the subphase is washed out so that any detrimental effect of solvent on the surface activity of the film is negligible.

The other limitation is that precision varied with the spreading pressure. For a spreading pressure greater than 45 mN/m, precision was high, as indicated by the small difference in area per molecule between rapid compression isotherms for DPPC film spread under identical conditions (Table 1), and by the close agreement of the rapid compression surface tension-area isotherms for DPPC film with those obtained at slow compression in another CBS (Schürch et al., 1989) and in a Wilhelmy balance (Goerke and Clements, 1986) (Fig. 2). However, for a spreading pressure less than 45 mN/m, precision was low. This finding is in contrast to those of Schürch et al. (1989) and Putz et al. (1994a). At the moment we do not have an explanation for this difference. This problem does not exclude spreading of film at spreading pressures less than 45 mN/m. However, if film has to be spread with high precision, at present we suggest working at high spreading pressures when this spreading technique is used.

In conclusion, the developed method allows routine formation of film by spreading of small amounts of surfactant components at the air-water interface of an air bubble with great ease and without the need for special equipment. Furthermore, it requires only small amounts of material while allowing biophysical activity testing of surfactant in a leak-proof surfactometer. Finally, because application of this technique to a comparative study of spread and adsorbed film showed that differences in surface activity are small, the developed method will be useful for mechanistic studies of surfactant protein-phospholipid interactions of spread film and comparative studies of adsorbed and spread film.

We thank Dr. Herbert Benzer for support of this study; Ing. Marcel Baum and Hubert Staud for help with construction of the CBS; Drs. Anton Amann, John A. Clements, Jon Goerke, and Steve Hall for suggestions with preparation of the manuscript; and Mimi Zeiger for editorial help.

This research was supported in part by funds from the Department of Anaesthesia and Intensive Care Medicine Innsbruck, the Netherlands Foundation for Chemical Research (S.O.N.) and the Netherlands Organization for Scientific Research (N.W.O.).

REFERENCES

Bartlett, G. R. 1959. Phosphorus assay in column chromatography. *J. Biol. Chem.* 234:466–468.

Bligh, E. G., and W. J. Dyer. 1959. A rapid method of total lipid extraction and purification. *Can. J. Biochem. Physiol.* 37:911–917.

Böhlen, P., S. Stein, W. Dairman, and S. Udenfriend. 1973. Fluorimetric assay of proteins in the nanogram range. *Arch. Biochem. Biophys.* 155:213–220.

Enhorning, G., B. Shumel, L. Keicher, J. Sokolowski, and B. A. Holm. 1992. Phospholipases introduced into the hypophase affect the surfactant film outlining a bubble. *J. Appl. Physiol.* 73:941–945.

Goerke, J., and J. A. Clements. 1986. Alveolar surface tension and lung surfactant. *In* Handbook of Physiology. American Physiological Society, Washington, DC. 247–261.

Goerke, J., and S. Schürch. 1997. Mechanical properties of the alveolar surface. *In* The Lung: Scientific Foundations. Lippincott-Raven, Philadelphia. 1169–1176.

Herold, R., H. Bünger, and U. Pison. 1996. Assessment of pulmonary surfactant function using a captive-bubble surfactometer. *Colloids Surf.* 114:211–219.

Holm, B. A., L. Keicher, M. Liu, J. Sokolowski, and G. Enhorning. 1991. Inhibition of pulmonary surfactant function by phospholipases. *J. Appl. Physiol.* 71:317–321.

Nag, K., J. Perez-Gil, A. Cruz, N. H. Rich, and K. M. W. Keough. 1996. Spontaneous formation of interfacial lipid-protein monolayers during adsorption from vesicles. *Biophys. J.* 71:1356–1363.

Oosterlaken-Dijksterhuis, M. A., H. P. Haagsman, L. M. G. Van Golde, and R. A. Demel. 1991. Characterization of lipid insertion into monomolecular layers mediated by lung surfactant proteins SP-B and SP-C. *Biochemistry.* 30:10965–10971.

Putz, G., J. Goerke, S. Schürch, and J. A. Clements. 1994a. Evaluation of pressure-driven captive bubble surfactometer. *J. Appl. Physiol.* 76: 1417–1424.

Putz, G., J. Goerke, H. W. Taeusch, and J. A. Clements. 1994b. Comparison of captive and pulsating bubble surfactometers with use of lung surfactants. *J. Appl. Physiol.* 76:1425–1431.

Qanbar, R., and F. Possmayer. 1995. On the surface activity of surfactant-associated protein C (SP-C): effects of palmitoylation and pH. *Biochim. Biophys. Acta.* 1255:251–291.

Schoel, W. M., S. Schürch, and J. Goerke. 1994. The captive bubble method for the evaluation of pulmonary surfactant: surface tension, area, and volume calculations. *Biochim. Biophys. Acta.* 1200:221–290.

Schürch, S., H. Bachofen, J. Goerke, and F. Possmayer. 1989. A captive bubble method reproduces the in situ behavior of lung surfactant monolayers. *J. Appl. Physiol.* 67:2389–2396.

Schürch, S., R. Quanbar, H. Bachofen, and F. Possmayer. 1995. The surface-associated surfactant reservoir in the alveolar lining. *Biol. Neonate.* 67:61–76.

Szoka, F., and D. Papahadjopoulos. 1980. Comparative properties and methods of preparation of lipid vesicles (liposomes). *Annu. Rev. Biophys. Bioeng.* 9:467–508.

Taneva, S., and K. M. Keough. 1994. Pulmonary surfactant proteins SP-B and SP-C in spread monolayers at the air-water interface. III. Proteins SP-B plus SP-C with phospholipids in spread monolayers. *Biophys. J.* 66:1158–1166.

Touchstone, J. C., J. C. Chen, and K. M. Beaver. 1980. Improved separation of phospholipids in thin layer chromatography. *Lipids.* 15:61–62.

Yu, S. H., and F. Possmayer. 1990. Role of bovine pulmonary surfactant-associated proteins in the surface-active property of phospholipid mixtures. *Biochim. Biophys. Acta.* 1046:233–241.